SECED 2023 Conference
*Earthquake Engineering & Dynamics for a Sustainable Future*
14-15 September 2023, Cambridge, UK

# DRIFT CAPACITY OF TEXTILE REINFORCED MORTAR MASONRY WALLS

Dan V. BOMPA[1] & Ahmed Y. ELGHAZOULI[2]

**Abstract**: *This paper examines the experimental drift response of unreinforced masonry (URM) strengthened with textile-reinforced mortar (TRM) overlays subjected to in-plane lateral cyclic displacements and axial compression. Comparative evaluations are carried out on a set of URM and TRM-strengthened wall counterparts collected from the literature in terms of main kinematics and drift parameters. URM walls include both regular and irregular masonry made of clay bricks or stone units, whilst the TRM incorporates polymeric or natural fibres in lime-based renders, representing material characteristics of various historic structures. The assessments undertaken in this study show that the drift capacity of URM walls is well estimated by code procedures. It is also shown that the double-sided TRM-strengthened walls can fail either in diagonal tension or flexure depending on the detailing and properties of the TRM. In addition to these modes, one-sided TRM-strengthened walls can also develop significant out-of-plane deformations in the post-peak. The ultimate drifts obtained through a bilinearisation procedure vary between 0.66-5.78% depending largely on the strengthening details, overlay thickness and URM compressive strength. The average TRM-strengthened-to-URM ultimate drift capacity ratio of the tests from the literature is 1.75. Although specific expressions to quantify the drift capacity of TRM-strengthened URM members are not available, the current provisions for reinforced masonry are suitable for estimating conservatively the ultimate drift capacity of TRM-strengthened masonry walls.*

## Introduction

Unreinforced masonry (URM) accounts for nearly 100% of historic structures, and above 70% of all buildings worldwide, being identified as the most vulnerable building stock as demonstrated by past earthquakes (Dolce et al., 2006). The URM performance is influenced by several factors such as the almost non-existent tensile strength of masonry components (such as mortar, bricks, or stone ashlars), irregular component geometry, and inadequate connections between horizontal and vertical elements (Messali et al., 2017). Failure in URM walls can occur through out- or in-plane mechanisms. Masonry structures with ineffective connections between walls, piers, horizontal floors, or vertical elements fail out-of-plane, including complete or partial wall overturning, overturning with one or two side wings, corner failure, strip overturning, and horizontal or vertical arch mechanisms (D'Ayala and Speranza, 2003). In-plane failure modes are either shear- or flexure-governed depending on the URM wall geometry, aspect ratio and boundary conditions. Shear failures are either characterised by inclined cracks, or by a sliding crack when a portion of the wall along a bed-joint slides horizontally under lateral loads. The diagonal shear and sliding strength of URM is greatly dependent on the mortar-brick interaction (Bompa and Elghazouli, 2020, 2021). Appropriate structural details such as anchors and ties can prevent out-of-plane failures, allowing the structure to be governed by the in-plane behaviour of the walls and diaphragm stiffness. Insufficient in-plane deformability can lead to collapse, thus, having adequate drift capacity is essential for masonry in seismic regions.

When existing structures are inadequate for seismic demands, they can be modified locally or globally through repair, strengthening, or full replacement of damaged or undamaged elements. This can involve adding new structural elements or using local strengthening methods, as well as introducing passive protection. Local strengthening methods to prevent in-plane failure modes include surface strengthening or strengthening by inserting elements. Surface strengthening involves mechanical attachment of reinforcing mesh embedded in mortar overlays or bonding of fibre reinforced polymer laminates using epoxy adhesives. The former includes conventional wire welded meshes embedded in mortar overlays or polymeric meshes referred to as textile reinforced mortar (TRM) overlays (Papanicolaou et al., 2011). TRM overlays enhance the in-plane

[1] Senior Lecturer, University of Surrey, Guildford, UK, d.bompa@surrey.ac.uk
[2] Professor, Imperial College London, UK

strength, stiffness, and ductility of clay brick URM walls (Torres et al., 2021; Elghazouli et al., 2023). The contribution of the TRMs to strength and drift capacity may be limited in cases when the overlay separates from the substrate or local debonding in areas of stress concentration (Gattesco et al., 2015). For URM walls exhibiting a flexure-governed failure, the TRM has limited influence on the structural response, but can improve the energy dissipation (Elghazouli et al., 2022). Quantification of deformability of TRM-strengthened walls is essential for evaluating the effectiveness of the strengthening system. Whilst models for assessing the stiffness and strength exist, explicit guidance for determining the in-plane drift capacity of masonry walls with TRM overlays are lacking. This study investigates the drift capacity of URM strengthened with TRM overlays under in-plane lateral cyclic displacements and axial compression, using a database of tests collated from the literature.

## Tests database

*Wall configurations*

The test database includes a total of 65 walls subjected to reversed cyclic lateral loading and axial load, from a total of 10 different testing programmes. The collected tests include laboratory experiments on URM and TRM-strengthened walls, but exclude diagonal compression tests which are considered here as material characterisation tests. The tests include URM walls incorporating lime or cement-lime mortar, and solid or frog fired clay bricks (Papanicolaou et al., 2011; Torres et al., 2021; Elghazouli et al., 2022; Garcia-Ramonda et al., 2022; Trochoutsou et al., 2022), stone units (Tomaževič et al., 2015; Gattesco et al, 2015; Ponte et al., 2023), rubble limestone bricks (Meriggi et al., 2022), and adobe bricks (Hračov et al., 2016). The TRM-strengthened walls include glass, carbon, basalt, flax, or polyester textile meshes, embedded in mortars made of lime, or cement-lime with or without fibres. With a main focus on shear-governed responses, out of the 65 tests reviewed, 36 had flexure-governed failures (e.g. Papanicolaou et al., 2011) or failed by TRM debonding (Gattesco et al, 2015), and are excluded from the investigation. Wall panels repaired only with grout injection and without TRM overlays were also disregarded herein.

| Author | ID | Type | l (mm) | h (mm) | t (mm) | Bricks (-) | Joint mortar (-) | $f_j$ (MPa) | $f_b$ (MPa) | $f_m$ (MPa) |
|---|---|---|---|---|---|---|---|---|---|---|
| Elghazouli et al., 2022 | WA-D | URM-O | 1910 | 1310 | 110 | clay | lime | 2.2 | 14.6 | 4.25 |
| Torres et al., 2021 | URM | URM-O | 3000 | 2000 | 230 | clay | lime | 10.4 | 17.2 | 4.9 |
| Garcia-Ramonda et al., 2022 | URM_1 | URM-O | 1270 | 1270 | 310 | clay | lime | 2.6 | 17.9 | 6.5 |
| Trochoutsou et al., 2022 | BW | URM-O | 1150 | 1085 | 102 | clay | cement lime | 2.1 | 24.4 | 6.0 |
| Tomaževič et al., 2015 | Control | URM-C | 1000 | 1500 | 500 | stone | lime | 3.3 | 220 | 1.1 |
| Meriggi et al., 2022 | UM | URM-C | 1200 | 1200 | 250 | lime-stone | lime | 4.2 | 74 | 15.6 |
| Ponte et al., 2023 | URM 1 & 2 | URM-A | 1200 | 1200 | 400 | stone | lime | 2.2 | 50 | 2.44 |

*Table 1. Details of URM walls*

*Masonry patterns*

Schematic representations of the masonry patterns are shown in Figure 1. Clay brick walls can be defined as regular masonry, whilst the stone masonry was either cut stone masonry with good bond or irregular stone masonry, with pebbles, erratic and irregular stone units. The latter two correspond to Typologies C and A, respectively, from current classification guidelines (Szabó et al., 2022). The details of the reference URM walls are shown in Table 1, and the TRM details of the strengthened walls and main results are given in Table 2. In the table, the specimen ID is the same as reported in the paper, the masonry type is defined as URM-x (x is O for clay bricks, A for irregular stone and C for cut stone). The parameter l, h and h are the length, height, and thickness of the wall, respectively. Parameters $f_j$, $f_b$ and $f_m$ are the joint mortar, brick unit, and masonry strengths, as obtained from tests, respectively. Additionally, Table 2 gives the details of

the strengthening materials. These are the textile and mortar type, the overlay mortar strength $f_r$, overlay thickness $t_r$, number of sides and layers per side, and the textile weight per square metre.


*Figure 1. Typical masonry patterns: (a) regular clay brick masonry, (b) cut stone with good bond, (c) irregular stone masonry, with pebbles, erratic and irregular stone units.*

*Distribution of parameters*

Figure 2 illustrates the distribution of the main parameters of the tests with shear-governed responses from the database. All tests were carried out in laboratory conditions under cyclic loading. The aspect ratio of the walls (height/length) was h/l=0.64-1.50 (Figure 2a), and about two thirds of the specimens had low masonry strength $f_m$<6 MPa (Figure 2b). In all cases the $f_m$ was obtained from standardised wallette tests, or walls smaller than the cyclic specimens. For the cyclic tests, the axial load ratio $\sigma/f_m$, in which σ is the stress corresponding to the applied axial load, was below $\sigma/f_m$ = 0.3 (Figure 2c). With regard to the masonry type, as shown in Figure 2d, 15 walls were regular made of clay brick masonry (Type O), 8 were from cut stone with good bond (Type C), and the remaining 6 were irregular stone masonry (Type A). From the total of 29 walls, 9 were reference URM, 9 strengthened with glass, 2 with carbon, 6 with basalt and 3 with flax textiles. The measured overlay mortar compressive strength was $f_r$=2.70-22.0 MPa. In some studies, TRM coupons were also tested to evaluate the uniaxial properties of the composite (Elghazouli et al., 2022; Trochoutsou et al., 2022).

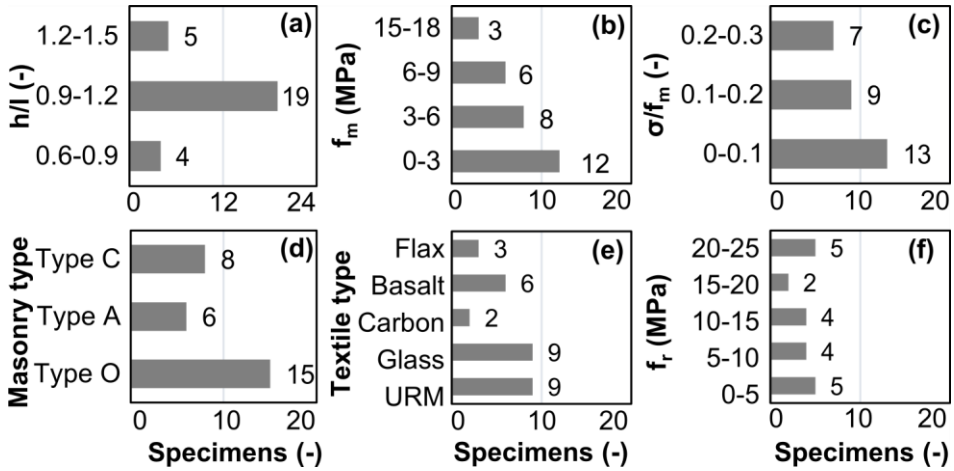


*Figure 2. Parameter distribution: (a) aspect ratio (h/l), (b) masonry comp strength ($f_m$), (c) axial load ratio ($\sigma/f_m$), (d) masonry pattern, (e) textile type, (f) compressive strength of mortar overlay.*

*Load-displacement response*

Test envelopes including the positive and negative branches were digitised using an open-source vector graphics programme from the reported test cyclic load-displacement (V-Δ) curves. From the complete envelope, the average of positive and negative curves, were bi-linearised considering the energy equivalence between the test and the bilinear idealisation, assuming that the effective stiffness intersects the test envelope at 70% of the peak lateral strength, i.e. $0.7\times V_{max}$ (Tomaževič 1999). The drift value $\Delta_u$ was defined as either the point at which the wall lateral strength decreased to 80% from $V_{max}$, or the highest drift value achieved during testing if this threshold was not reached (Figure 3). The ultimate strength $V_u$ corresponds to the maximum lateral strength from the bilinear representation and using the procedure described above. Figures 4, 5 and 6 illustrate the average test envelopes and bilinear curves of the specimens that had shear-governed responses. Table 2 depicts the main test parameters.

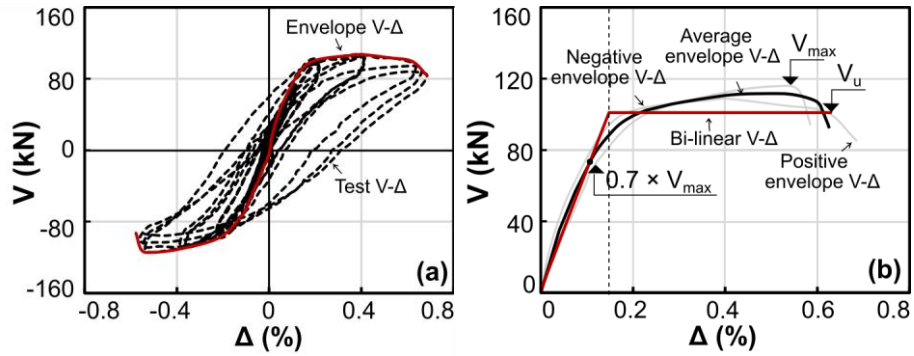


*Figure 3. (a) Force-displacement V-Δ (Elghazouli et al., 2021), (b) Bi-linearisation procedure*

## Experimental behaviour

*Clay brick masonry walls*

Single leaf masonry walls 3000 × 2000 × 230 mm³ (l × h × t) were tested to assess the effectiveness of TRM reinforcement (Torres et al., 2021). One wall was left unreinforced, one was damaged and repaired with TRM (DRW), and another was reinforced with TRM prior to testing (NDRW). The TRM reinforcement improved the strength, ductility, stiffness, and energy dissipation capacity of the walls without any mesh debonding. The capacity of the reinforced walls increased by 148% and 186% compared to the URM, as shown in Figure 4a. TRM also increased the displacement capacity of the walls, with final drift amplitudes increasing by 35% and 20% in the damaged and non-damaged reinforced walls, respectively. The damaged and repaired wall had higher energy dissipation capacity due to the previous damage causing the TRM to take all the load and degrade further.

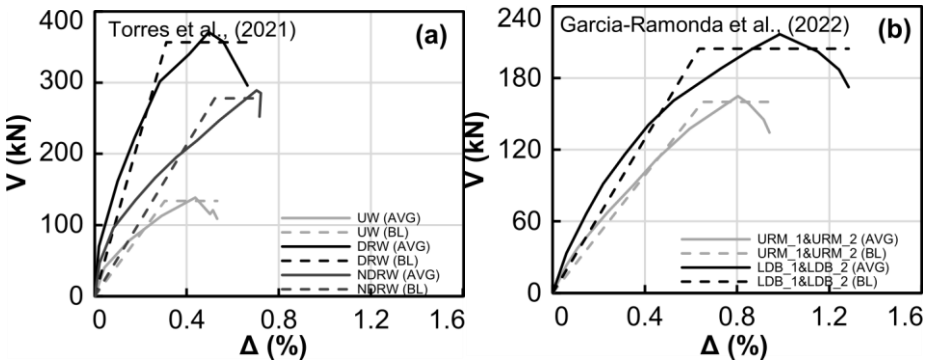


*Figure 4. V-Δ curves: (a) Torres et al (2021), (b) Garcia-Ramonda et al (2022)*

From four double leaf 1270×1270×310 mm³ (l × h × t) walls tested by Garcia-Ramonda et al. (2022), two were unreinforced (URM), two were repaired with grout and strengthened with basalt TRM (URM_R), and two were undamaged and strengthened with basalt TRM (LDB). The URM specimens showed diagonal cracking, while the LDB specimens had mixed responses. No toe crushing was observed. The TRM allowed the specimens to withstand larger loads and displacements, with all strengthened specimens showing increased lateral strength and drift capacity. The LDB specimens had an average increase of 30% and 34%, respectively (Figure 4b). Testing was stopped before the vertical residual capacity was lost.

Six medium-scale single-leaf masonry walls, with nominal size of 1125×1115x102 mm³ (l × h × t), were cyclically loaded in-plane, with one provided with a mortar overlay without textile meshes (LW), and four strengthened on both sides using one (FL1W) or two layers (FL2W) of flax textiles embedded in lime-based mortar (Trochoutsou et al., 2022). All walls failed in diagonal tension, with the URM wall experiencing significant damage at low drift levels. The flax reinforcement ensured the integrity of the wall and controlled the development of brittle failure modes. The strengthened walls showed improved in-plane strength and ultimate drift (up to 118%), as well as energy dissipation capacity. Increasing the reinforcement ratio from one to two textile layers resulted in a substantial enhancement in deformability (20%), but not in a directly proportional increase in in-plane strength (Figure 5a). The use of two TRM layers promoted a more effective distribution of strains across the wall.

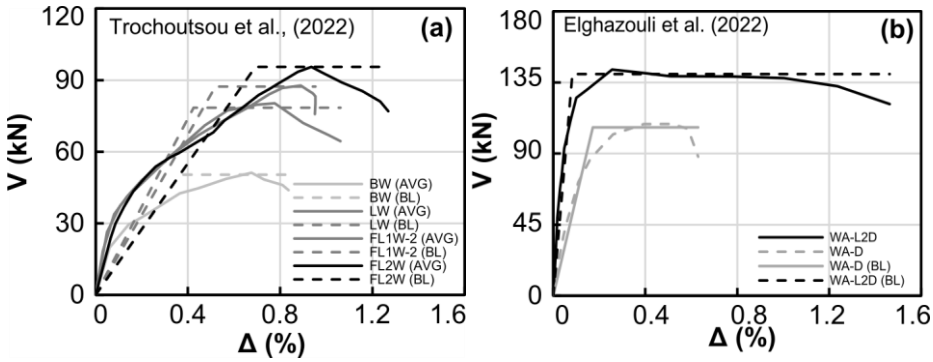


*Figure 5. V-Δ curves: (a) Trochoutsou et al., (2022), (b) Elghazouli et al., (2022)*

A comparison was made between a TRM-strengthened (WA-L2D) and a non-strengthened URM wall (WA-D) of 1910×1300×110 mm$^3$ (l × h × t) (Elghazouli et al., 2022). The URM walls failed in diagonal tension, but the addition of TRM overlays restricted diagonal crack development, resulting in a shift to rocking behaviour. The ultimate response was governed by gradual crushing at the toes during load reversals, combined with gradual buckling of the textile reinforced mortar overlay. The TRM overlay improved stiffness by 167% and increased strength by 30.6% compared to the non-rendered counterpart (Figure 5b). In the TRM-strengthened wall, there was a shift from URM diagonal tension to toe crushing, leading to a 132% increase in ultimate drift.

*Stone masonry walls*

Stone masonry walls with dimensions of 1500×1000×500 mm$^3$ (l × h × t) were tested under cyclic in-plane lateral loads at a constant axial load (Tomaževič et al., 2015). The study included two unreinforced walls and four TRM-strengthened walls, with glass textile meshes embedded in cement mortar overlay. All walls failed in diagonal tension. The strengthened walls exhibited a significant increase in lateral resistance compared to the unreinforced walls, with up to 2.5-4.0 times the resistance (Figure 6a). The degree of improvement did not depend on the type of coating but on the technology of application. The coating increased the rigidity of the walls, while also improving the displacement and energy dissipation capacities.

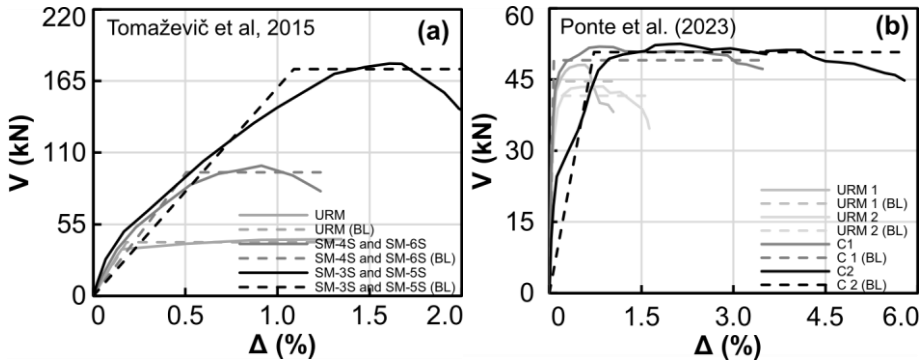


*Figure 6. V-Δ curves: (a) Tomaževič et al., 2015, (b) URM and glass TRM (Ponte et al., 2023)*

Two limestone masonry walls (1200×1200×250 mm$^3$) were tested by Meriggi et al. (2022). One was unreinforced (UM), while the other was rendered (PM). Both were strengthened with basalt textile externally bonded with a lime mortar (UM-R and PM-R). The TRM prevented diagonal tension, triggered a rocking/toe-crushing mechanism, and restored the strength, stiffness, and ductility of the damaged wall. The addition of transverse connectors prevented a leaf separation failure mechanism. The TRM contribution was negligible as the textile was not anchored at the base of the wall. Twelve 1200x1200x400 mm$^3$ specimens of lime mortar rubblestone masonry, including two URM walls, were used to evaluate the effectiveness of textile reinforced mortar systems with glass and carbon meshes. Only one layer of mesh, anchored in the walls with glass fibre connectors, was applied to one side of the walls (Ponte et al., 2023). The URM were severely damaged with large diagonal cracks due to shear failure on both sides of the specimens. The TRM overlay did not significantly increase the lateral strength due to weak wall to foundation interface. However, the reinforcement techniques changed the failure mode from shear to flexure resulting in a significant increase in lateral drift capacity above 4.0% (Figure 6b). Some specimens showed an out-of-plane behaviour and separation of the two leaves at the base.

## Drift capacity

*Unreinforced masonry*

In general, the lateral load-deformation (P-Δ) response of URM walls can be represented by an idealised bi-linear curve, as described above, or a piecewise linear relationship with due account for strength degradation (Tomaževič 1999; CEN, 2021a). For piecewise curves, such as that proposed in Eurocode 8-3, (CEN, 2021a), a bilinear representation can be considered to the yield drift $\Delta_y$, where the first branch, up to 70% of the peak strength, is given by the elastic stiffness $K_{el}$, whilst the second branch is 50-75% of $K_{el}$. A constant value of strength is assumed between the yield drift $\Delta_y$ and ultimate drift $\Delta_u$. A descending branch is then considered to a 'second' ultimate drift $\Delta_{u2}$, with a slope depending on the governing mechanism (i.e. flexure, sliding, diagonal tension). Regardless of the failure mode, the 'second' ultimate drift $\Delta_{u2}$ is assumed as 4/3 of $\Delta_u$ (i.e. $\Delta_{u2} = 1.33 \times \Delta_u$). The limits $\Delta_u$ and $\Delta_{u2}$ are considered to correspond to the Significant Damage and Near Collapse limit states, respectively. A schematic representation is shown in Figure 7a.

For diagonal failures, shown in Figure 7a, $\Delta_{d,u}$=0.6% for regular (stair-stepped joints) and $\Delta_{d,u}$=0.5% for irregular masonry, again with $\Delta_{d,u2}=1.33\Delta_d$. The residual shear force corresponding to $\Delta_{d,u2}$ is 50% of the shear resistance for regular masonry and 30% for irregular masonry. Only for completeness, shear sliding and flexure-controlled drift limits are mentioned here. For shear sliding failures of historic (pre-modern) masonry, a value of $\Delta_{s,u}$=0.8% is stipulated while, when shear sliding is limited by masonry unit strength, $\Delta_{s,u}$=0.5% is suggested, with $\Delta_{s,u2}=1.33\Delta_{s,u}$. The residual shear strength corresponding to $\Delta_{s,u2}$ is that estimated from a Mohr-Coulomb representation without considering the contribution of the initial shear strength (CEN, 2021a). In the revised Eurocode 8-3 (CEN, 2021a), for elements failing in flexure, $\Delta_{f,u}$=0.01(1-v), where v is the normalised axial load ratio described before and $\Delta_{f,u2}=1.33\Delta_{u,f}$ corresponds to a reduction of 10% in shear force for regular masonry and 20% for irregular masonry in the post-peak regime. According to current Eurocode 8-3 (CEN, 2005a), for flexure-controlled walls, the ultimate drift $\Delta_{f,u}=0{,}008 \cdot h_0/d$, and for all shear-governed cases $\Delta_{v,u}$=0.40%.

*Strengthened masonry.*

According to Eurocode 8-1-2 (CEN, 2021b), the drift capacity of reinforced masonry may be assumed as 1.5 times those of URM, unless demonstrated otherwise by tests whilst, according to Eurocode 8-3 (CEN, 2021a), the deformation capacity is 1.33 the URM, provided that detailing is compatible with Eurocode 6 (CEN, 2005b) recommendations. The $1.33\text{-}1.50 \times \Delta_{d,u}$ (for diagonal tension) is shown in Figure 7b. ASCE 41-17 (2017) provides a wide range of drift limits for reinforced masonry walls under in-plane actions depending on the aspect ratio, reinforcement ratio, axial load, and a residual strength ratio. The second drift in Eurocode 8-3, $\Delta_{u2}$ and associated strength, can be correlated with the drift and corresponding strength obtained by applying the residual strength ratio in ASCE 41-17 (2017). These drifts vary within 0.2%-2.6% as a function of the wall aspect ratio, reinforcement ratios, and axial load. For shear-governed walls with axial load ratios above 0.15, the element is 'force-controlled'.

As shown above, deformation limits exist in seismic assessment and retrofitting codes (Eurocode 8-3, ASCE41-17). However, these are for masonry reinforced by steel rebars, and cannot be applied directly to URM strengthened with TRM overlays. Although TRM-specific recommendations acknowledge the enhancement in deformation capacity, they do not provide expressions to quantify the deformation capacity of TRM-strengthened URM. A direct comparison between the test drift capacity of masonry walls strengthened with basalt TRM, and those from the current Eurocode 8-3 and other codes for URM, indicated that both standards underestimate the deformation capacity both at SD and NC (Garcia-Ramonda et al., 2022). This points to the need for specific limits for TRM-strengthened masonry.

As illustrated in Figure 7a with dashed red curves, the average ultimate drift capacity $\Delta_u$ of all clay brick URM walls (regular Type O) is $\Delta_u$=0.78%, whilst for the stone masonry URM walls (Types A & C) is $\Delta_u$=1.21% (Table 2). The average for the entire dataset is $\Delta_u$=0.97%. It is shown that these values exceed the code limits both for regular (stair-stepped joints) and irregular masonry. With respect to the TRM-strengthened walls, the $\Delta_u$ of all clay brick walls (regular Type O) is $\Delta_u$=1.19%, and for stone walls is $\Delta_u$=2.61%, with an overall average of $\Delta_u$=1.82%. This is shown in dashed green curves. Comparatively, the code range for $\Delta_u$ obtained by multiplying $\Delta_{d,u}$=0.6% for regular (stair-stepped joints) by the 1.33 and 1.5 factors is also shown in grey colour. Overall, it is shown that the code limits are conservative, both for URM and for TRM-strengthened walls, when the reinforced masonry assumption is used.

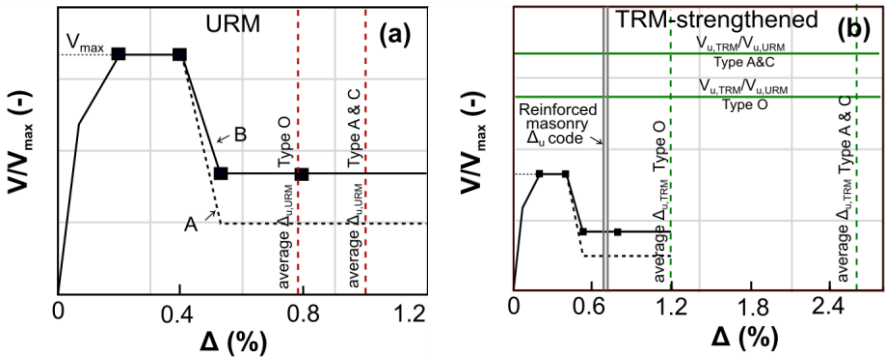


*Figure 7. (a) V-Δ relationships for URM controlled by diagonal cracking (A irregular masonry, B regular masonry) and comparison with database $\Delta_u$, (b) URM V-Δ, code $\Delta_u$ for reinforced masonry, and database average $\Delta_u$ and $V_u$ of TRM-strengthened walls.*

*TRM-strengthened to URM drift capacity ratio.*

Based on the experimental response described in previous sections, the in-plane behaviour of a TRM- strengthened wall can be divided into three main stages: linear-elastic, cracked, and post-peak. During the pre-peak stage, the contribution of the textile is limited, and the stiffness enhancement mainly comes from the mortar overlay. After the masonry cracking, the TRM is activated, acting as a crack-bridging mechanism that limits crack widths and delays failure. Global or local debonding can govern the response when the overlay-substrate interface properties are weak, and the overlay cannot develop its tensile strength. Moreover, poor mortar-textile bond can lead to mesh slip from the mortar matrix. Global debonding involves a leaf separation mechanism when the overlay de-bonds from the substrate (Gattesco et al., 2015). Local debonding is activated by stress localisation such as at the wall toes (Elghazouli et al., 2023). In such situations, TRM overlays on both wall sides can modify the in-plane resisting mechanism, by preventing a diagonal tension-controlled response and triggering rocking/toe-crushing (Meriggi et al., 2022). For single-sided TRM-strengthened walls, in-plane diagonal tension and toe crushing, and out-of-plane bending, can develop (Ponte et al., 2023).

Provided that the TRM is adequately bonded and anchored in the masonry wall, a TRM-strengthened wall has superior drift capacity, regardless of the governing mode. This is supported by the TRM-strengthened-to-URM ultimate drift capacities ($\Delta_{u,TRM}/\Delta_{u,URM}$) shown in Table 2 and the average ratios in Figure 8. It is shown that the average $\Delta_{u,TRM}/\Delta_{u,URM}$=1.75 which is above the ranges suggested in the revised Eurocode 8-3 (CEN, 2021b). For the clay brick masonry (Type O) the average ratio is $\Delta_{u,TRM}/\Delta_{u,URM}$=1.50, and is explained by either cracking of the TRM in diagonal tension with significant strains in the textile, e.g. Specimens DRW and NDRW (Torres et al., 202), or shift to a flexural mode, e.g. Specimen WA-L2D (Elghazouli et al., 2022), both providing ductility to the system. For the stone masonry walls (Types A and C) the average ratio is $\Delta_{u,TRM}/\Delta_{u,URM}$=2.06. Note that in some cases the TRM-strengthened walls had $\Delta_{u,TRM}$ comparable to $\Delta_{u,TRM}$. For the single-side TRM strengthened Specimens SM-4S and SM-6S, some out-of-plane deformation may have developed leading to leaf separation (Tomaževič et al, 2015), as was the case for Specimen C1 (Ponte et al., 2023) although it had very high $\Delta_{u,TRM}$ due to flexure.

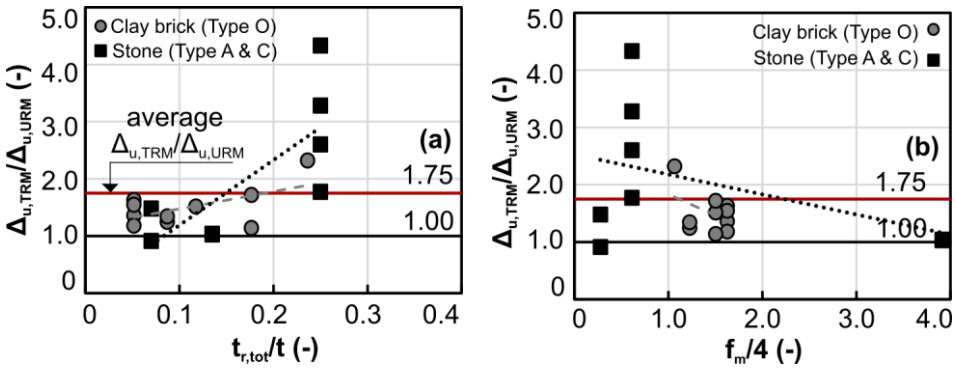


*Figure 8. Relationship between the $\Delta_{u,TRM}/\Delta_{u,URM}$ ratio and: (a) total overlay thickness-to-URM thickness ratio ($t_{r,tot}/t$), (b) crushing limit stress ($f_m/4$)*

| ID | WT* (-) | OM (-) | $f_r$ (MPa) | $t_r$ (mm) /S | S (-) | TL (-) | W (g/ $m^2$) | N (kN) | $V_{max}$ (kN) | FM** (-) | $\Delta_y$ (%) | $\Delta_u$ (%) | $\Delta_{u,TRM}/\Delta_{u,URM}$ (-) |
|---|---|---|---|---|---|---|---|---|---|---|---|---|---|
| WA-D | U | none | 0 | 0 | 0 | 0 | - | 227.3 | 110.6 | DT | 0.15 | 0.63 | - |
| WA-L2D | G | lime cement | 20.4 | 13.0 | 2 | 2 | 160 | 224.2 | 143.1 | | 0.08 | 1.46 | 2.30 |
| URM | U | none | | | 0 | 0 | - | 150.0 | 139.0 | DT | 0.30 | 0.53 | - |
| DRW* | G | lime fibres | 18.8 | 10.0 | 2 | 1 | 225 | 150.0 | 340.0 | DT | 0.31 | 0.66 | 1.25 |
| NDRW | G | lime fibres | 18.8 | 10.0 | 2 | 1 | 225 | 150.0 | 340.0 | DT | 0.52 | 0.72 | 1.35 |
| URM_1 | U | none | 0 | 0 | 0 | 0 | - | 118.0 | 172.0 | DT | 0.66 | 0.86 | - |
| URM_2 | U | none | 0 | 0 | 0 | 0 | - | 118.0 | 157.0 | DT | 0.64 | 1.02 | - |
| URM1_R* | B | lime | 12.9 | 8.0 | 2 | 1 | 200 | 118.0 | 179.0 | DT | 0.55 | 1.28 | 1.36 |
| URM2_R* | B | lime | 12.9 | 8.0 | 2 | 1 | 200 | 118.0 | 182.0 | DT | 0.63 | 1.54 | 1.63 |
| LDB_1 | B | lime | 12.9 | 8.0 | 2 | 1 | 200 | 118.0 | 211.0 | DT | 0.75 | 1.46 | 1.55 |
| LDB_2 | B | lime | 12.9 | 8.0 | 2 | 1 | 200 | 118.0 | 222.0 | DT | 0.52 | 1.11 | 1.18 |
| BW | U | none | 0 | 0 | 0 | 0 | | 70.0 | 51.0 | DT | 0.37 | 0.84 | - |
| FL1W-2 | F | lime fibres | 2.7 | 9.0 | 2 | 2 | 300 | 70.0 | 88.0 | DT | 0.52 | 0.95 | 1.14 |
| FL2W-1 | F | lime fibres | 2.7 | 6.0 | 2 | 1 | 300 | 70.0 | 96.0 | DT | 0.69 | 1.27 | 1.52 |
| FL2W-2 | F | lime fibres | 2.7 | 9.0 | 2 | 2 | 300 | 70.0 | 103.0 | DT | 0.79 | 1.44 | 1.72 |
| Control | U | cement | | | 0 | 0 | | 163.8 | 45.2 | DT | 0.18 | 1.35 | |
| SM-4S | G | cement | 22 | 17.5 | 1 | 1 | 280 | 163.8 | 141.2 | DT | 0.50 | 1.23 | 0.92 |
| SM-6S | G | cement | 22 | 17.5 | 1 | 1 | 280 | 163.8 | 105.9 | DT | | | |
| SM-3S | G | cement | 22 | 17.5 | 2 | 1 | 280 | 163.8 | 160.3 | DT | 1.09 | 2.00 | 1.48 |
| SM-5S | G | cement | 22 | 17.5 | 2 | 1 | 280 | 163.8 | 179.3 | DT | | | |
| UM | U | none | 0 | 0 | 0 | 0 | | 180.0 | 121.0 | DT | 0.45 | 0.83 | - |
| UM-R** | B | lime | 4.1 | 16.9 | 2 | 1 | 250 | 180.0 | 153.0 | LS | 0.45 | 0.85 | 1.03 |
| PM-R** | B | lime | 4.1 | 16..9 | 2 | 1 | 250 | 180.0 | 174.0 | OTC | 0.50 | 0.81 | 1.04 |
| URM 1 | U | lime | | | 0 | 0 | | 144.0 | 48.7 | DT | 0.07 | 1.04 | - |
| URM 2 | U | lime | | | 0 | 0 | | 144.0 | 44.1 | DT | 0.08 | 1.63 | - |
| G1 | G | lime | 9.7 | 50.0 | 1 | 1 | 52 | 144.0 | 52.9 | DT/TC | 0.25 | 2.37 | 1.80 |
| G2 | G | lime | 9.7 | 50.0 | 1 | 1 | 52 | 144.0 | 54.7 | DT/TC | 0.07 | 4.38 | 3.30 |
| C1 | C | lime | 9.7 | 50.0 | 1 | 1 | 374 | 144.0 | 52.8 | DT/TC /OP | 0.07 | 3.47 | 2.60 |
| C2 | C | lime | 9.7 | 50.0 | 1 | 1 | 374 | 144.0 | 53.4 | DT/TC /OP | 0.7 | 5.78 | 4.30 |

Legend: WT – Wall type; OT – Overlay mortar; S – Overlay sides, TL – Textile layers per side, W – Textile weight in g/$m^2$, FM – Failure mode.
*WT: U – URM, C – Carbon TRM, G – Glass TRM, B – Basalt TRM, F – Flax TRM
**FM: DT - Diagonal tension, OTC - Onset of toe-crushing, LS - Leaf separation, TC - Toe crushing, OP - Out of plane

*Table 2. Details of the TRM-strengthened walls and main results.*

The drift capacity appears proportional to the overlay thickness, as illustrated in Figure 8a through the $t_{r,tot}/t$ ratio ($t_{r,tot}$ is total overlay thickness, and t is the URM wall thickness). Conversely, the drift capacity is indirectly proportional to the strut crushing stress ($f_m/4$ in which $f_m$ is the masonry compressive strength) as shown in Figure 8b. This expression is similar to that adopted in Eurocode 6 as an upper limit for reinforced masonry beams subjected to shear loading (CEN, 2005b). For double-sided TRM strengthening, having a relatively low $f_m$ means that toe-crushing is likely to govern. As rocking/toe-crushing is inherently a more ductile mechanism than diagonal tension, the drift capacity is also greater (Figure 8b). With regard to codified procedures, as stipulated in Eurocode 8-1-2 (CEN, 2021b) and Eurocode 8-3 (CEN, 2021a), the drift capacity of

reinforced masonry members may be assumed as 1.5 times and 1.33 times those of URM, respectively, unless other values are demonstrated by tests and provided that details are compatible with those in Eurocode 6 (CEN, 2005b). Considering the database $\Delta_{u,TRM}/\Delta_{u,URM}$=1.75 from Table 2, it is shown that that the current provisions are suitable for estimating the ultimate drift capacity of TRM-strengthened masonry walls.

## Conclusions

The paper examined the experimental drift response of unreinforced masonry (URM) strengthened with textile-reinforced mortar (TRM) overlays. The URM walls included regular and irregular masonry made of clay bricks or stone units, representing material characteristics of various historic structures, and the TRM incorporated polymeric or natural fibres in lime-based renders. Comparative evaluations were carried out on a set of URM and TRM-strengthened wall counterparts collected from the literature in terms of main kinematics and drift parameters. The main remarks are outlined below.

- The double-sided TRM-strengthened walls could fail either in diagonal tension or flexure depending on the detailing and properties of the TRM. One-sided TRM-strengthened walls could also develop significant out-of-plane deformations in the post-peak. TRMs can maintain the in-plane diagonal tension response to ultimate, but also modify it triggering the rocking/toe-crushing mechanisms.
- TRMs typically enhance the rigidity of the walls and ensure the integrity of the wall controlling the development of brittle failure modes. A higher number of TRM layers per side promote a more effective strain distribution, resulting in enhanced seismic performance with higher energy dissipation capacity. The presence of the TRM allows for the redistribution of stress, resulting in the masonry withstanding comparatively larger loads and displacements.
- The enhancement in performance primarily depends on the technology of application, rather than the type of overlay. The addition of transverse connectors to the TRM can prevent local mechanisms such as local TRM buckling or global mechanisms such as complete TRM debonding or leaf separation that may occur in URMs. The contribution of the strengthening is almost negligible if the textile was not anchored at the base of the wall.
- The assessments showed that the drift capacity of URM walls was well estimated by code approaches. The ultimate drifts of TRM-strengthened walls obtained through a bilinearisation procedure varied between 0.66-5.78% depending largely on the strengthening details, overlay thickness and URM compressive strength. The average TRM-strengthened-to-URM ultimate drift capacity ratio of the tests from the literature was 1.75.
- Although specific expressions to quantify the drift capacity of TRM-strengthened URM members were not available, the current provisions for reinforced masonry were suitable for estimating conservatively the ultimate drift capacity of TRM-strengthened masonry walls.

## References

ASCE (American Society of Civil Engineers), 2017. ASCE/SEI 41-17 Seismic Evaluation and Retrofit of Existing Buildings. ASCE (American Society of Civil Engineers). Reston, Virginia

Bompa, D.V. and Elghazouli, A.Y., 2020. Experimental and numerical assessment of the shear behaviour of lime mortar clay brick masonry triplets. Construction and Building Materials, 262, p.120571. doi: 10.1016/j.conbuildmat.2020.120571

Bompa, D.V. and Elghazouli, A.Y., 2021. Mechanical properties of hydraulic lime mortars and fired clay bricks subjected to dry-wet cycles. Construction and Building Materials, 303, p.124458. doi: 10.1016/j.conbuildmat.2021.124458

CEN (European Committee for Standardization), 2004. EN 1998-1: 2004: Eurocode 8: Design of structures for earthquake resistance. Part 1: General rules, seismic actions and rules for buildings. European Committee for Standardisation, Brussels.

CEN (European Committee for Standardization), 2005a. EN 1998-3: 2005: Eurocode 8. Design of Structures for Earthquake Resistance. Assessment and Retrofitting of Buildings. European Committee for Standardisation, Brussels.

CEN (European Committee for Standardization), 2005b. EN 1996-1-1: 2005 Eurocode 6: Design of masonry structures—General rules for reinforced and unreinforced masonry structures. European Committee for Standardisation, Brussels.

CEN (European Committee for Standardization), 2021a. Eurocode 8: Design of structures for earthquake resistance – Part 3: Assessment and retrofitting of buildings and bridges. European Committee for Standardisation, Brussels.

CEN (European Committee for Standardization), 2021b. Eurocode 8: Design of structures for earthquake resistance — Part 1-2: Rules for new buildings. European Committee for Standardisation, Brussels.

D'Ayala, D. and Speranza, E., 2003. Definition of collapse mechanisms and seismic vulnerability of historic masonry buildings. Earthquake Spectra, 19(3), pp.479-509. doi: 10.1193/1.1599896

Dolce, M., Kappos, A., Masi, A., Penelis, G. and Vona, M., 2006. Vulnerability assessment and earthquake damage scenarios of the building stock of Potenza (Southern Italy) using Italian and Greek methodologies. Engineering Structures, 28(3), pp.357-371. doi: 10.1016/j.engstruct.2005.08.009

Elghazouli, A.Y., Bompa, D.V., Mourad, S.A. and Elyamani, A., 2021. In-plane lateral cyclic behaviour of lime-mortar and clay-brick masonry walls in dry and wet conditions. Bulletin of Earthquake Engineering, 19(13), 5525-5563. doi: 10.1007/s10518-021-01170-5

Elghazouli, A.Y., Bompa, D.V., Mourad, S.A., Elyamani, A., 2022. Seismic Performance of Heritage Clay Brick and Lime Mortar Masonry Structures. In: Vacareanu, R., Ionescu, C. (eds) Progresses in European Earthquake Engineering and Seismology. ECEES 2022. Springer, Cham. doi: 10.1007/978-3-031-15104-0_14

Elghazouli, A.Y., Bompa, D.V., Mourad, S.A. and Elyamani, A., 2023. Ultimate in-plane shear behaviour of clay brick masonry elements strengthened with textile reinforced mortar overlays. Technical Report. Imperial College London.

Garcia-Ramonda, L., Pelà, L., Roca, P. and Camata, G., 2022. Cyclic shear-compression testing of brick masonry walls repaired and retrofitted with basalt textile reinforced mortar. Composite Structures, 283, p.115068. doi: 10.1016/j.compstruct.2021.115068

Gattesco, N., Amadio, C. and Bedon, C., 2015. Experimental and numerical study on the shear behavior of stone masonry walls strengthened with GFRP reinforced mortar coating and steel-cord reinforced repointing. Engineering Structures, 90:143-157. doi: 10.1016/j.engstruct.2015.02.024

Meriggi, P., Caggegi, C., Gabor, A. and de Felice, G., 2022. Shear-compression tests on stone masonry walls strengthened with basalt textile reinforced mortar (TRM). Construction and Building Materials, 316, p.125804. doi: 10.1016/j.conbuildmat.2021.125804

Messali, F., Metelli, G. and Plizzari, G., 2017. Experimental results on the retrofitting of hollow brick masonry walls with reinforced high-performance mortar coatings. Construction And Building Materials, 141, pp.619-630. doi: 10.1016/j.conbuildmat.2017.03.112

Papanicolaou, C., Triantafillou, T. and Lekka, M., 2011. Externally bonded grids as strengthening and seismic retrofitting materials of masonry panels. Construction and Building Materials, 25(2), pp.504-514. doi: 10.1016/j.conbuildmat.2010.07.018

Ponte, M., Penna, A. and Bento, R., 2023. In-plane cyclic tests of strengthened rubble stone masonry. Materials and Structures, 56(2), pp.1-18. doi: 10.1617/s11527-023-02126-8

Szabó, S., Funari, M.F. and Lourenço, P.B., 2023. Masonry patterns' influence on the damage assessment of URM walls: Current and future trends. Developments in the Built Environment, p.100119. doi: 10.1016/j.dibe.2023.100119

Tomaževič, M., 1999. Earthquake-resistant design of masonry buildings. Imperial College.

Tomaževič, M., Gams, M. and Berset, T., 2015. Strengthening of stone masonry walls with composite reinforced coatings. Bulletin of Earthquake Engineering, 13, pp.2003-2027. doi: 10.1007/s10518-014-9697-7

Torres, B., Ivorra, S., Baeza, F.J., Estevan, L. and Varona, B., 2021. Textile reinforced mortars (TRM) for repairing and retrofitting masonry walls subjected to in-plane cyclic loads. An experimental approach. Engineering Structures, 231, p.111742. doi: 10.1016/j.engstruct.2020.111742

Trochoutsou, N., Di Benedetti, M., Pilakoutas, K. and Guadagnini, M., 2022. In-Plane Cyclic Performance of Masonry Walls Retrofitted with Flax Textile–Reinforced Mortar Overlays. Journal of Composites for Construction, 26(5), p.04022049. doi: 10.1061/(ASCE)CC.1943-5614.0001238